Geometry and dynamics in the fractional discrete Fourier transform

Kurt Bernardo Wolf and Guillermo Krötzsch

Instituto de Ciencias Físicas, Universidad Nacional Autónoma de México, Cuernavaca, Morelos 62251, México

The $N \times N$ Fourier matrix is one distinguished element within the group $\mathsf{U}(N)$ of all $N \times N$ unitary matrices. It has the *geometric* property of being a fourth root of unity and is close to the *dynamics* of harmonic oscillators. The dynamical correspondence is exact only in the $N \to \infty$ contraction limit for the *integral* Fourier transform and its fractional powers. In the finite-N case, several options have been considered in the literature. We compare their fidelity in reproducing the classical harmonic motion of discrete coherent states. © 2007 Optical Society of America

OCIS codes: 070.2590, 070.6020, 030.1670.

1. INTRODUCTION

The integral Fourier transform (IFT) participates in the foundations of quantum mechanics and is ubiquitous in signal processing. Geometrically, the IFT is a fourth root of unity; its fractionalization is not unique, but one distinguished fractional IFT (FrIFT)[1] is the one-parameter cyclic subgroup $\mathsf{U}(1)$ of the Lie group $\mathsf{Sp}(2,\mathsf{R})$ of linear canonical transformations in one-dimensional quantum mechanics,[2] describing the time evolution of the quantum harmonic oscillator (see, e.g., Ref. 3, Part IV). Its applications to optics include the paraxial wave model,[4] and in signal processing these have been widely documented by Ozaktas *et al.*[5] Here we examine analog finite structures that satisfy both the geometry of the FrIFT as fourth roots of unity and the dynamics of discrete coherent states as finite counterparts of the classical and quantum-mechanical harmonic motion.

The discrete Fourier transform (DFT) is *approximately* realized in planar multimodal optical or acoustical paraxial waveguides[6] and in symmetric one-lens setups,[7–9] where the input signal is produced by a linear array of N-emitting points (with controlled phases) and measured by a similar array of sensors. A corresponding fractional DFT (FrDFT) occurs for any length along the guide or for spaces around the lens setup. In the literature we find several approaches to define a FrDFT (five of which we review in this paper), presenting various computational and mathematical advantages. Although we refrain from selecting a "best" FrDFT, we compare different versions in terms of their rendering of the motion of coherent states.

In Section 2 we recall some of the remarkable properties of the FrIFT, its integral kernel, and its relation with the harmonic oscillator wave functions and coherent states. The DFT matrix $\mathbf{F}$ and a standard modulo-4 fractionalization of any fourth root of unity are presented in Section 3. In Section 4 we fractionalize the powers α of $\mathbf{F}^\alpha$ determined by Fourier eigenbases V; these are all one-parameter cyclic groups of matrices $\mathbf{F}_V^\alpha \in \mathsf{U}(1)_V \subset \mathsf{U}(N)$

that pass through $\mathbf{F}$ and its integer powers. We also propose a simple analog definition of coherent states. The time evolution of these states is explored computationally in Section 5 for the "Taipei" basis of Pei and Yeh[10] and Pei *et al.*,[11] the eigenbasis of Mehta,[12] and the "Ankara" basis of Candan, Ozaktas, and coauthors[13,14] (see also Ref. 5, Chap. 4). As expected, coherent states of low energy have Gaussianlike shapes and oscillate harmonically; differences between the models arise only at high energies. In Section 6 we briefly recall the "Cuernavaca" Fourier–Kravchuk transform and its coherent states.[6,15,16] A succinct concluding Section 7 ends the discussion.

2. FrIFT AND THE HARMONIC OSCILLATOR

There exists a close relation between the IFT operator $\mathcal{F}$ acting on the Hilbert space $\mathcal{L}^2(\mathsf{R})$ of quantum mechanics and the harmonic oscillator evolution at one-quarter period [Ref. 3, Eq. (7.197)],

$$\mathcal{F} = e^{i\pi/4} \exp\left[-i\tfrac{1}{4}\pi(\mathcal{P}^2 + \mathcal{Q}^2) \right], \tag{1}$$

where we have the Schrödinger operators of position $(\mathcal{Q}{:}f)(x) := xf(x)$ and momentum $(\mathcal{P}{:}f)(x) := -i\mathrm{d}f(x)/\mathrm{d}x$, and where $e(i\pi/4)$ is the *metaplectic* phase (Ref. 17, Appendix C). This leads to the definition of the *fractional* IFT operators $\mathcal{F}^\alpha$ through a *number* operator $\mathcal{N}$,

$$\mathcal{F}^\alpha := \exp\left(-i\tfrac{1}{2}\pi\alpha\mathcal{N}\right), \quad \mathcal{N} := \tfrac{1}{2}(\mathcal{P}^2 + \mathcal{Q}^2) - \tfrac{1}{2}\mathbf{1}. \tag{2}$$

The spectrum of $\mathcal{N}$ in $\mathcal{L}^2(\mathsf{R})$ is $k \in \{0, 1, 2, \dots\}$, nondegenerate, and $\mathcal{F}^4 = 1$ is the unit operator. The normalized eigenfunctions of $\mathcal{N}$ are the well-known quantum harmonic oscillator functions,

$$\Psi_k(x) = \exp\left(-\tfrac{1}{2}x^2\right)H_n(x) / \sqrt{2^k k! \sqrt{\pi}}. \tag{3}$$

The ground state is $\Psi_0(x)$, and there is no "top" state.

Acting on functions $f \in \mathcal{L}^2(\mathsf{R})$, $\mathcal{F}^\alpha$ is a unitary integral transform that one can write, using either powers or angles $\phi := \tfrac{1}{2}\pi\alpha$, as

$$(\mathcal{F}^\alpha{:}f)(x) = \int_{\mathsf{R}} dx' F^{(\alpha)}(x,x') f(x'), \tag{4}$$

$$F^{(\alpha)}(x,x') = \frac{e^{i\phi/2}}{\sqrt{2\pi i \sin\phi}} \exp i \frac{(x^2 + x'^2)\cos\phi - 2xx'}{2\sin\phi} \tag{5}$$

$$= \sum_{k=0}^{\infty} \Psi_k(x)\exp(-ik\phi)\Psi_k(x')^*. \tag{6}$$

In the closed-form Eq. (5), the square root is understood to be $\sqrt{is} := \exp(i\tfrac{1}{2}\pi\,\mathrm{sign}\,s)\sqrt{|s|}$, and there are Dirac singularities at $F^{(0)}(x,x') = \delta(x-x') = F^{(4)}(x,x')$ and $F^{(2)}(x,x') = \delta(x+x')$. The bilinear generating function form of Eq. (6) (Ref. 18) exposes the role of the orthonormal and complete oscillator basis $\Psi_k(x)$ in Eq. (3), which are eigenfunctions of $\mathcal{F}$ with the four infinitely degenerate eigenvalues, $(-i)^k \in \{1, -i, -1, i\}$.

The probability density of the oscillator functions, $|\Psi_k(x)|^2$, are the *invariants* under α-evolution. Functions that are *covariant* should have one parameter undergoing harmonic motion; these are the coherent states, which can be defined equivalently as ground states displaced by a complex parameter c, or as linear generating functions of the oscillator functions, also with powers of c,

$$\Upsilon_c(x) := e^{c^2/2}\Psi_0(x - \sqrt{2}c) \tag{7}$$

$$= \sum_{k=0}^{\infty} \frac{c^k}{\sqrt{k!}}\Psi_k(x). \tag{8}$$

The evolution cycle of $\Upsilon_c(x)$ under $\mathcal{F}^\alpha$ is evinced in the harmonic motion of the parameter $c(\alpha)$,

$$\mathcal{F}^\alpha \Upsilon_{c(0)}(x) = \Upsilon_{c(\alpha)}(x), \quad c(\alpha) = c(0)\exp\left(-i\tfrac{1}{2}\pi\alpha\right). \tag{9}$$

3. DISCRETE FOURIER TRANSFORM

The standard $N \times N$ DFT matrix is $\mathbf{F} = \|F_{m,m'}\|$, with elements that involve powers of the Nth roots of unity,

$$F_{m,m'} := \frac{1}{\sqrt{N}}\exp\left(-i\frac{2\pi mm'}{N}\right). \tag{10}$$

It is periodic ($F_{m,m'} = F_{m+kN,m'} = F_{m,m'+k'N}$ for k, k' integers), symmetric ($F_{m,m'} = F_{m',m}$), and unitary ($\mathbf{F}^\dagger\mathbf{F} = \mathbf{1} = \mathbf{F}\mathbf{F}^\dagger$), so $|\det\mathbf{F}| = 1$. Its square is the inversion matrix $(\mathbf{F}^2)_{m,m'} = \delta_{m,-m'}$, and $\mathbf{F}^4 = \mathbf{1}$ is a fourth root of the unit matrix.

A. Eigenvalues and Projectors
The eigenvalues of the $N \times N$ standard DFT matrix are the fourth roots of unity, to be denoted by $\varphi(n) := (-i)^n = \exp(-i\tfrac{1}{2}\pi n) \in \{1, -i, -1, i\}$, for $n \in \{0,1,2,3\}$. This divides the space of N-point complex signals into four Fourier-invariant subspaces whose dimensions N_φ are the multiplicities of the eigenvalues φ, which have a peculiar modulo-4 recurrence in the dimension $N =: 4J + n$, given by

Dimension	Multiplicities N_φ				
N	$\varphi = 1$	$-i$	-1	i	$\det\mathbf{F}$
$4J$	$J+1$	J	J	$J-1$	$-i(-1)^J$
$4J+1$	$J+1$	J	J	J	$(-1)^J$
$4J+2$	$J+1$	J	$J+1$	J	$-(-1)^J$
$4J+3$	$J+1$	$J+1$	$J+1$	J	$i(-1)^J$

$$\tag{11}$$

for $J > 0$, i.e., roughly $N_\varphi \approx \tfrac{1}{4}N$; of course $\Sigma_\varphi N_\varphi = N$. These Fourier subspaces are mutually orthogonal; their projector matrices are

$$\mathbf{P}_\varphi = \frac{1}{4}\sum_{n=0}^{3}\varphi^{-n}\mathbf{F}^n, \quad \mathbf{F}^n = \sum_\varphi \varphi^n\mathbf{P}_\varphi, \tag{12}$$

satisfying $\mathbf{P}_\varphi\mathbf{P}_{\varphi'} = \delta_{\varphi,\varphi'}\mathbf{P}_\varphi$.

B. Standard Fractionalization
Fourth roots of unity, such as $\mathbf{F}$, have "standard" fractional powers $\mathbf{F}_{\mathrm{S}}^\alpha$ that we consider to be purely geometrical. They are given by

$$\mathbf{F}_{\mathrm{S}}^\alpha := \sum_{n=0}^{3}\exp\left(i\tfrac{3}{4}\pi(n-\alpha)\right)\frac{\sin\pi(n-\alpha)}{4\sin\tfrac{1}{4}\pi(n-\alpha)}\mathbf{F}^n \tag{13}$$

$$= \exp\left(-i\tfrac{1}{2}\pi\alpha\mathbf{N}_{\mathrm{S}}\right), \quad \mathbf{N}_{\mathrm{S}} := \sum_{n=0}^{3}n\mathbf{P}_{\varphi(n)}. \tag{14}$$

They satisfy composition, $\mathbf{F}_{\mathrm{S}}^\alpha\mathbf{F}_{\mathrm{S}}^\beta = \mathbf{F}_{\mathrm{S}}^{\alpha+\beta}$, and Eq. (13) ensures that for integer $\alpha = n$, $\mathbf{F}_{\mathrm{S}}^n = \mathbf{F}^n$. This $\mathsf{U}(1)_{\mathrm{S}}$ Lie group is displayed in Eq. (14) as generated by a "number matrix" $\mathbf{N}_{\mathrm{S}}$, in the same form as in Eq. (2). The Fourier eigenspaces with eigenvalues $\varphi(0) = 1$, $\varphi(1) = -i$, $\varphi(2) = -1$, and $\varphi(3) = i$ are also eigenspaces of the number matrix with eigenvalues $n = 0, 1, 2, 3$, respectively.

However simple and universal the standard FrDFT [Eq. (13)] appears to be, it is *not* the fractionalization we want to consider, because while for $N \to \infty$ the DFT matrix (10) contracts to the IFT kernel $e^{-ixx'}/\sqrt{2\pi}$, the standard FrDFT matrix (13) does *not* contract to the canonical integral transform kernel (5), belonging to the continuous FrIFT group on $\mathcal{L}^2(\mathsf{R})$.

4. FRACTIONALIZATION OF DFT IN A BASIS V

The last paragraph justifies considering a number matrix *different* from the standard $\mathbf{N}_{\mathrm{S}}$ in Eq. (14). Its spectrum should be $k \in \{0, 1, \ldots, N-1\}$ and increase only the interval $[0, N]$ under contraction $N \to \infty$.

A. Fourier Eigenbases and Their FrDFTs
Within each φ-subspace one can find orthonormal bases V of N-column vectors, which we indicate by $\mathbf{v}^{(\varphi,j)} = \|v_m^{(\varphi,j)}\|$, labeled by $j \in \{0, 1, \ldots, N_\varphi - 1\}$, and with rows $m \in \{1, 2, \ldots, N\}$. They will satisfy

$$\mathbf{v}^{(\varphi,j)\dagger}\mathbf{v}^{(\varphi',j')} = \delta_{\phi,\varphi'}\delta_{j,j'}, \quad \sum_{j=0}^{N_\varphi-1}\mathbf{v}^{(\varphi,j)}\mathbf{v}^{(\varphi,j)\dagger} = \mathbf{P}_\varphi \qquad (15)$$

and can be arranged in four $N \times N_\varphi$ rectangular matrices $\mathbf{V}^{(\varphi)} = \|v_m^{(\varphi,j)}\|$. There are slight and nonessential differences in the expressions of the four φ-cases in Eq. (11); we shall not need their explicit forms.

Next we build the bilinear generating function analogous to Eq. (6) for the finite bases V characterized above. For noninteger α we must further specify that $\varphi^\alpha \equiv (\varphi(n))^\alpha := \exp(-i\frac{1}{2}\pi n\alpha)$ with $n \in \{0,1,2,3\}$. We define the V-FrDFT by the $N \times N$ matrices $\mathbf{F}_V^\alpha$, whose elements are

$$(\mathbf{F}_V^\alpha)_{m,m'} := \sum_{\varphi(n)}\sum_{j=0}^{N_\varphi-1}v_m^{(\varphi,j)}\exp\left[-i\frac{1}{2}\pi(4j+n)\alpha\right]v_{m'}^{(\varphi,j)*} \quad (16)$$

$$= \sum_\varphi \varphi^\alpha(\mathbf{V}^{(\varphi)}\mathbf{\Phi}^{(\varphi)}(\alpha)\mathbf{V}^{(\varphi)\dagger})_{m,m'}, \qquad (17)$$

$$\mathbf{\Phi}^{(\varphi)}(\alpha) := \mathrm{diag}(\exp(-2i\pi j\alpha)) \text{ is } N_\varphi \times N_\varphi. \qquad (18)$$

The last line defines the matrix $\mathbf{\Phi}^{(\varphi)}(\alpha)$, which is diagonal and independent of φ—except for its dimension. The conditions of Eq. (15) ensure the multiplication property $\mathbf{F}_V^\alpha\mathbf{F}_V^\beta = F_V^{\alpha+\beta}$ modulo 4, and the unitarity $(\mathbf{F}_V^\alpha)^\dagger = \mathbf{F}_V^{-\alpha}$, of each set of V-FrDFT matrices. When α is integer, $\mathbf{\Phi}^{(\varphi)}(\alpha) = \mathbf{1}$, and the matrix (17) becomes the sum of the projectors in Eq. (12), so $\mathbf{F}_V^n = \mathbf{F}^n$. The V-FrDFT matrices thus belong to subgroups $\mathsf{U}(1)_V \subset \mathsf{U}(N)$, all of which pass through the standard DFT matrix and its integer powers.

B. Number Matrix of an Eigenbasis
Note that in each φ-subspace, the numbering of the N_φ basis vectors $\mathbf{v}^{(\varphi,j)}$ by $j \in \{0,1,\ldots,N_\varphi-1\}$ is arbitrary; our construction is still purely geometric, since no dynamic "energy spectrum" is used to suggest any prefered order. (Three bases will be examined in the next section.) Starting with one V basis, represented by the $N \times N$ matrix $\mathbf{V}$, we can subject each φ-subspace to an $N_\varphi \times N_\varphi$ unitary transformation $\mathbf{U}^{(\varphi)} \in \mathsf{U}(N_\varphi)$, so that through right multiplication we obtain a new W-basis associated to the product of matrices $\mathbf{W} = \mathbf{V}\mathbf{U}$ as well as a new one-parameter cyclic group of W-FrDFTs that will also pass through the standard DFT matrix $\mathbf{F}$ and its integer powers. The manifold of these $\mathsf{U}(1)_V$ FrDFT subgroups within the N^2-dimensional manifold of $\mathsf{U}(N)$ has dimension $\Sigma_\varphi N_\varphi^2$ and can be characterized by its tangent at the origin, namely, its number matrix.

The V-FrDFT matrix in Eqs. (16)–(18) has the form of Eq. (2) in continuous systems; they are Lie exponentials of an $N \times N$ *number* matrix associated to the basis V,

$$\mathbf{F}_V^\alpha = \exp\left(-i\frac{1}{2}\pi\alpha\mathbf{N}_v\right),$$

$$\mathbf{N}_V := i\frac{2}{\pi}\frac{d}{d\alpha}\mathbf{F}_V^\alpha\bigg|_{\alpha=0}, \qquad (19)$$

$$= \sum_{\varphi(n)}\sum_{j=0}^{N_\varphi-1}\mathbf{v}^{(\varphi,j)}\,\mathrm{diag}(4j+n)\mathbf{v}^{(\varphi,j)\dagger}. \qquad (20)$$

The eigenvectors of the number matrix are $\mathbf{v}^{(\varphi(n),j)}$ with nondegenerate eigenvalues $4j+n \in \{0,1,2,\ldots,N-1\}$. Finally, note that the number operator in Eqs. (19) and (20) can serve equally well to define the V-FrDFT group of matrices proposed in Eqs. (16)–(18).

C. Discrete Coherent States
The requirement that the bilinear generating function form of the V-FrDFT proposed in Eq. (16) contract in the $N \to \infty$ limit to the FrIFT in Eq. (6) suggests that we should propose discrete or discretized oscillatorlike functions, numbered by $k = 4j+n$ as above, to have "good" V-bases for the fractionalization of the DFT matrix $\mathbf{F}$. The three models of the next section comprise essentially identical low-lying eigenvectors, and they differ most sharply in the highest ones. The FrDFTs of sampled functions, such as centered rectangles,[10,11] do not provide a sufficient and reliable impression of their overall fidelity to the FrIFT. Our proposal here is to examine the existence and behavior of associated coherent states.

Associated to the V-FrDFT in Eq. (16), we search for states given by N-vectors $\Upsilon_c^V(m)$ that contract to the continuous coherent states $\Upsilon_c(x)$ in Eqs. (7) and (8). This can be made by truncating the infinite sum to the N available functions or by displacing the ground state. The latter can be done when the system is periodic and has a well-identified ground state $(j,n) = (0,0)$. For generic, nonperiodic V-bases, we opt for the former choice, Eq. (8), defining discrete coherent states as linear generating functions of the V-basis vectors, namely, as N-point column vectors of components

$$\Upsilon_c^V(m) = \sum_{\varphi(n)}\sum_{j=0}^{N_\varphi-1}\frac{c^{4j+n}}{\sqrt{(4j+n)!}}v_m^{(\varphi,j)}. \qquad (21)$$

When multiplied on the left by $\mathbf{F}_V^\alpha$, each summand is multiplied by a phase that is collected by the complex parameter $c(\alpha) = c(0)\exp(-i\frac{1}{2}\pi\alpha)$, exactly as in Eq. (9), so that the V-FrDFT is a uniform rotation of the complex c-plane. For "arbitray" bases V, the vectors defined by Eq. (21) may not mean much, but for "good" bases (closely related to the oscillator wave functions), the discrete coherent state $\mathbf{Y}_c^V$ should initially resemble a displaced Gaussian and should oscillate as its continuous counterparts without undue distorsion.

5. APPROACHES TO DISCRETE OSCILLATOR DYNAMICS
Since the FrIFT has close connection with the dynamics of the quantum harmonic oscillator, so should their

V-FrDFT analogs. In this section we describe three approaches: two of them based on the oscillator wavefunctions $\Psi_k(x)$ in Eq. (3), and one based on *importing* symmetry to a discrete and concrete physical model.

A. Sampled Harmonic Oscillator: Taipei Bases

It is suggestive to build bases for *V*-FrDFTs using *sampled* oscillator functions $\Psi_k(x_m)$ in Eq. (3). Pei and Yeh[10] and Pei *et al.*,[11] working in Taipei, have constructed FrDFTs defined through the bilinear generating function (16). They first define the vectors $\boldsymbol{\phi}^{(k)}$, $k \in [0, N-1]$,

$$\phi_m^{(k)} := \Psi_k\left(\sqrt{\frac{2\pi}{N}}m\right), \quad \text{where} \qquad (22)$$

$$m \in \begin{cases} \left[-\frac{1}{2}N, \frac{1}{2}N - 1\right] & N \text{ even} \\ \left[-\frac{1}{2}(N-1), \frac{1}{2}(N-1)\right] & N \text{ odd} \end{cases} . \qquad (23)$$

These *N*-vectors are not quite orthogonal, except for parity $(-1)^k$ (we call this the *uncorrected* Taipei basis); they are not naturally periodic in k nor m, unless so defined beyond their natural range; and they are not guaranteed to have k changes of sign in m as the continuous functions do. However, they do provide an *approximate* FrDFT when replaced directly in Eq. (16), which produces credible harmonic motion on its coherent states.

We display the uncorrected Taipei basis $\phi_m^{(k)}$ by the gray-tone matrix (m, k) in Fig. 1; there we can see the relative signs and the regions where the components are near zero. The errors are small in this uncorrected basis for the lower-lying states. For example, when $N = 33$ as in our figures, the maximum of the overlaps $(\boldsymbol{\phi}^{(k)}, \boldsymbol{\phi}^{(k')})$ for $k \neq k' \leq 22 = \frac{2}{3}N$ is 0.01. The coherent states constructed according to Eq. (21), with the uncorrected Taipei basis (23) are shown in Fig. 2 for three values of $c(0)$, over one-quarter of the Fourier cycle. The center of the Gaussian-like bumps is at $m_{\max}(\alpha) \approx \sqrt{N/\pi}\,\text{Re}\,c(\alpha)$; in the figure, for $N = 33$, the peak of a $c = 5$, coherent state is at $m_{\max} = 16.2$, just outside the interval $m \in [-16, 16]$, yet it oscillates quite harmonically and does not unduly disperse.

The refinement of this construction constitutes the work of Pei and Yeh[10] and Pei *et al.*,[11] who first projected the basis functions (22) by Eq. (12) to separate them into the four φ-eigenspaces and then applied a modified Gramm–Schmidt computer orthonormalization process within each eigenspace, with the numbering provided naturally by the energy quantum label k.

B. Mehta Eigenbasis

We consider next a (previous and) very elegant basis for FrDFTs given by Mehta in 1987,[12] who found that the sums of periodically displaced oscillator functions (3),

$$\mu_m^{(k)} = \mu_{m+N}^{(k)} := \sum_{s=-\infty}^{\infty} \Psi_k\left(\sqrt{\frac{2\pi}{N}}(m + Ns)\right), \qquad (24)$$

are *N* eigenvectors of the DFT matrix, $\mathbf{F}\boldsymbol{\mu}^{(k)} = (-\mathrm{i})^k \boldsymbol{\mu}^{(k)}$, which (as the Taipei basis) is not *quite* orthogonal. Except for orthogonality, this Mehta basis also fulfills most expectations of Eq. (16) with $k = 4j + n$; appears in Fig. 3. Comparison with Fig. 1 shows that they differ only at the

highest values of energy k. The coherent states built out of the *Mehta basis* are shown in Fig. 4; since they are periodic, for large c they "spill over" the ends of the interval at $\pm\frac{1}{2}(N-1)$.

Generalizations of these *Mehta functions* to other similarly summed Fourier eigensets of special functions have been shown by Atakishiyev and others[19,20] to extend into the much wider field of discrete *q*-special functions.

C. Ankara Lattice and FrDFT

A group of researchers and students based in Ankara introduced, by analogy with continuous systems, the Hamiltonian for a periodic vibrating lattice model.[13,14] This system consists of *N* points of equal mass, numbered cyclically by $m \in \{1, 2, \ldots, N \equiv 0\}$, that are on a circle, joined to their equilibrium positions and to one another by springs. The states of the system are given by the *N* complex quantities $\{f_m(\tau)\}$ subject to time-τ Schrödinger evolution by a real Hamiltonian matrix $\mathbf{H}_A = \|H_{m,m'}^A\|$ (A for Ankara); solving a difference equation, the solution is a Green matrix $\mathbf{G}_A(\tau)$,

$$\mathbf{H}_A\mathbf{f}(\tau) = \mathrm{i}\frac{\mathrm{d}}{\mathrm{d}\tau}\mathbf{f}(\tau) \Leftrightarrow \mathbf{f}(\tau) = \mathbf{G}_A(\tau)\mathbf{f}(0), \qquad (25)$$
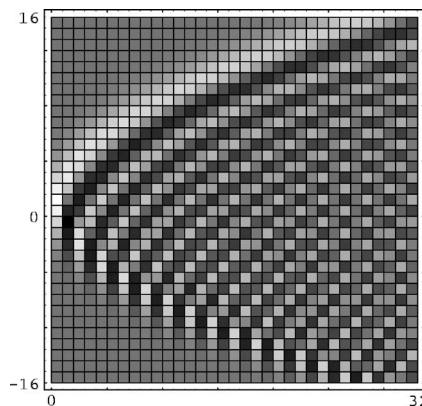

Fig. 1.   Matrix (m, k) of the uncorrected Taipei basis $\varphi_m^{(k)}$ of sampled oscillator functions in Eq. (22) for $N = 33$. Light and dark elements indicate positive and negative values, respectively.
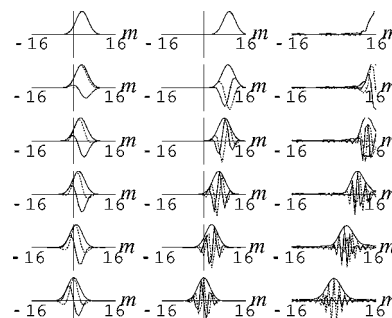

Fig. 2.   Motion of coherent states built out of the uncorrected Taipei basis of sampled oscillator functions in Eq. (22) for $N = 33$. In the three columns $c(0) = 1, 3, 5$. The rows show their evolution over a quarter-period for $\alpha = 0, 0.2, \ldots 1.0$. Dashed curve, real parts; dotted curve, imaginary parts; solid curve, absolute values.
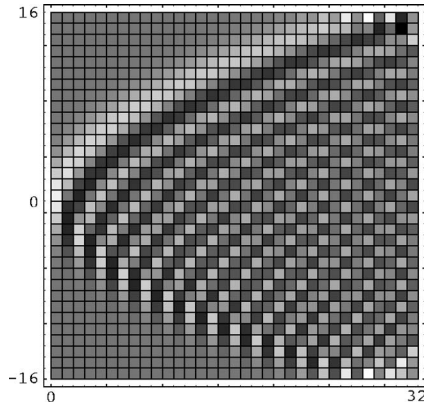
Fig. 3. Matrix (m,k) of the Mehta of oscillator functions $\mu_m^{(k)}$ in Eq. (24). It differs significantly from that in Fig. 1 only in the highest k-columns.
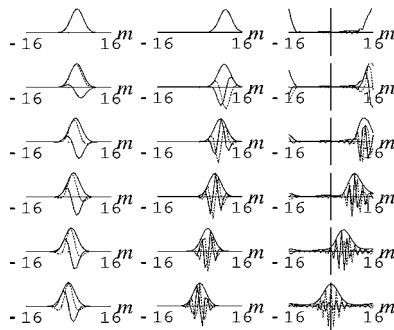

Fig. 4. Motion of Mehta coherent states built out of the basis $\mu_m^{(k)}$ in Eq. (24). The rows and columns have the same parameters as those in Fig. 2.

$$\mathbf{G}_A(\tau) := \exp(-i\tau\mathbf{H}_A). \qquad (26)$$

The τ-evolution of the lattice defines a group of "A-transforms" that is expected to lie approximately on an A-FrDFT closed cycle (still to be defined), i.e.,

$$\mathbf{F}_A^{\alpha(\tau)} \approx \exp[-i\tau(\mathbf{H}_A - h_0\mathbf{1})]. \qquad (27)$$

Here h_0 is the lowest (*vacuum*) energy; this is an analog of the metaplectic phase correction in Eqs. (1) and (2) in the continuous case.

The group in Ankara[5,13,14] considered the natural difference analog of Eq. (2),

$$\mathbf{H}_A := -\tfrac{1}{2}(\mathbf{\Delta} + \widetilde{\mathbf{\Delta}}), \qquad (28)$$

$$\mathbf{\Delta} := \mathrm{circ}(-2,1,0,\ldots,0,1), \qquad (29)$$

$$\widetilde{\mathbf{\Delta}} := \mathbf{F}\mathbf{\Delta}\mathbf{F}^{-1} = \mathrm{diag}(-4\sin^2(\pi m/N)). \qquad (30)$$

This Hamiltonian contains the kinetic energy of the circulating second-difference matrix $\mathbf{\Delta}$, which is due to equal springs between first neighbors along the circle. The potential energy is contained in the springs that tie each mass to its equilibrium position by the diagonal $\widetilde{\mathbf{\Delta}}$, soft around $m \approx N \equiv 0$ and stiff around $m \approx \tfrac{1}{2}N$.

As in the continuous case, the Ankara oscillator system in Eq. (28) is invariant under the DFT; $\mathbf{F}$ and $\mathbf{H}_A$ can be simultaneously diagonalized with a common set of eigenvectors,

$$\mathbf{H}_A\mathbf{h}^{(k)} = E_k\mathbf{h}^{(k)}, \quad \mathbf{F}\mathbf{h}^{(k)} = \varphi(n)\mathbf{h}^{(k)}, \qquad (31)$$

where the numeration follows that of Eq. (16) with $k = 4j + n$. The *energy* eigenvalues $\{E_k\}$ are the roots of an Nth degree polynomial; they are real and nondegenerate (except for one double degeneracy when N is a multiple of 4^{13}), and they are naturally ordered in k by the number of sign alternations in m. Yet they are not equally spaced nor rational nor algebraic (for $N > 4$), so they have to be computed numerically. The $h_m^{(k)}$'s have been named Harper functions;[14] they are *bona fide* orthonormal and periodic N-point signals; their matrix is shown in Fig. 5 (cf. Figs. 1 and 3).

D. Importation of Symmetry

The time evolution of the Ankara lattice is produced by the Green matrix in Eq. (26), whose matrix elements are the bilinear generating functions

$$G_{m,m'}^A(\tau) = \sum_{k=0}^{N-1} h_m^{(k)}\exp(-i\tau E_k)h_{m'}^{(k)}. \qquad (32)$$

The Green matrix is unitary for all $\tau \in \mathsf{R}$; but since the $\{E_k\}$ are not commensurable, the τ-line of Green matrices does *not* close into a $\mathsf{U}(1)$ circle but is a Lissajous-type curve in the N^2-dimensional manifold of $\mathsf{U}(N)$.
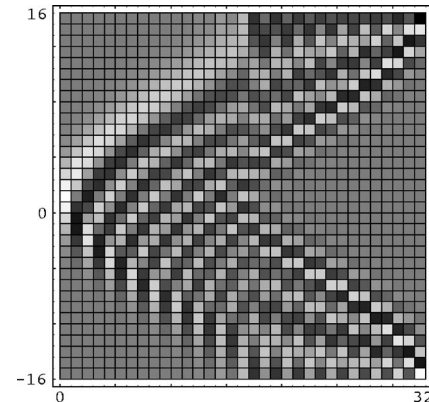
To produce a FrDFT with a modulo-4 cycle, the Ankara

Fig. 5. Matrix (m,k) of the Ankara oscillator with the Harper functions $h_m^{(k)}$. Note the "jump" at $k \approx 1/2N$ between states where the soft springs contain most of the energy and those where the lattice vibration is largest in the stiff zone.
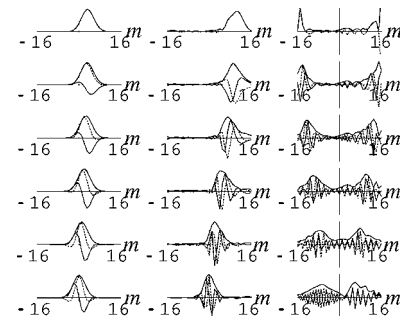

Fig. 6. Motion of coherent states built out of the Harper functions $h_m^{(k)}$ of the Ankara oscillator [Eq. (31)] with imported symmetry. The parameters are the same as in Figs. 2 and 4. In the last column we see the effect of the stiff-mode dominance.

group *imported* the symmetry of the continuous system by replacing the physical spectrum $\{E_k\}$ of the vibrating lattice with the linear number spectrum $\{k\}$ between 0 and $N-1$. The action of this A-FrDFT on the Harper coherent states, defined as in Eq. (21) is shown in Fig. 6. For large c, the stiff modes at the interval ends overwhelm the soft modes, so most of the energy lingers there throughout the cycle.

Symmetry importation has maintained dialogue with many of the works on finite models of quantum mechanics[21–24] and discrete models with number-phase uncertainty relations.[25–28] Here, the importation of symmetry both evinces and bridges the gap between the dynamics of the physical system on one hand and the geometric requirement of a fractional DFT generated by a number matrix.

E. Discrete Toroidal and Plane Phase Spaces
In order to associate a phase space to discrete systems along the lines of continuous classical or quantum Hamiltonian systems, we must put in place proper definitions of position and momentum; such may also be based on the dynamics of coherent states, although we should be prepared for mismatches between the two.

The simplest analogy consists in assigning to the row numbers of the state N-vectors $\mathbf{f}=\|f_m\|$ the meaning of discrete position, and to the row numbers of its DFT $\mathbf{Ff}=\|\tilde{f}_{m'}\|$ the meaning of discrete momentum. Their intertwining by $\mathbf{F}$ implies that these discrete sets of points should be considered periodic with the period N, so phase space is a discrete torus of points (m,m'). Integer translations along the position or momentum circles are well defined, as well as a discrete Heisenberg–Weyl group with a phase composition, and a discrete Wigner function can also be defined[29–31] with the most important properties of its continuous counterpart. On this construction, however, understanding the role of the *fractional* DFT is difficult, because classically it is supposed to rotate the position circle continuously onto the momentum circle—in spite of the topological obstruction presented by the hole of the torus.

Discrete coherent states $\mathbf{Y}_c^V$ as defined in Eq. (21) provide for another picture of phase space, namely, the complex c-plane, whose real and imaginary parts take the role of continuous position and momentum variables. The action of the FrDFT is then in complete accordance with classical expectations but collides with the notion that the phase space of discrete systems should be compact.

6. su(2) FINITE OSCILLATOR MODEL
A discrete, finite system with the geometry *and* dynamics of the harmonic oscillator was proposed in Ref. 6 (see also Ref. 16), realized as a planar paraxial, shallow multimodal waveguide that processes N-point complex signals in parallel, and produced and received at linear arrays of point emitters and sensors. This model, developed in Cuernavaca, follows with a "discrete quantization" of the classical harmonic oscillator. It has natural coherent states whose behavior was analyzed in Ref. 15. Here we highlight only the main postulates and results in terms

comparable to the models of Section 5.

A. Position, Momentum, and Number
Discretely quantized, the classical observables of position q and momentum p are assigned *not* to the eigenvalues of the Schrödinger operators $\mathcal{Q}$ and $\mathcal{P}$ seen above, *but* to the eigenvalues of the operators $\mathcal{L}_i$ of the Lie algebra of angular momentum and spin su(2), which is characterized by $\vec{\mathcal{L}}\times\vec{\mathcal{L}}=i\vec{\mathcal{L}}$. The new asignments (with overbars) and their spectra are

$$\text{position: } \bar{\mathcal{Q}}\leftrightarrow\mathcal{L}_x, \quad m\in\{-l,-l+1,\ldots,l\}, \quad (33)$$

$$\text{momentum: } \bar{\mathcal{P}}\leftrightarrow\mathcal{L}_y, \quad p\in\{-l,-l+1,\ldots,l\}, \quad (34)$$

$$\text{number: } \bar{\mathcal{N}}\leftrightarrow\mathcal{L}_z+l\mathbf{1}, \quad k\in\{0,1,\ldots,2l\}, \quad (35)$$

within the spin-l representation of su(2), for fixed $l\in\{0,\frac{1}{2},1,\ldots\}$. This representation has dimension $N=2l+1$, as determined by the quadratic Casimir operator,

$$\bar{\mathcal{Q}}^2+\bar{\mathcal{P}}^2+(\bar{\mathcal{N}}-l\mathbf{1})^2=l(l+1)\mathbf{1}. \quad (36)$$

B. Eigenvectors of Number
The signals sensed along the waveguide evolve through a discrete version of the FrIFT, the fractional *Fourier–Kravchuk* transform (FrFKT), which is built exactly as in Eq. (2), but with the number operator $\bar{\mathcal{N}}$ in Eq. (35). It is a rotation around the z axis that carries the position x axis onto the momentum y axis. The basis $\psi_k^{(l)}$ of the FrFKT are the eigenvectors of the number operator $\mathcal{L}_z$, measured in the position basis of $\mathcal{L}_x$, and are known as the Wigner little-d functions [Ref. 32, Eq. (3.65)],

$$\psi_k^{(l)}(m)=d_{m,k-l}^l\left(-\tfrac{1}{2}\pi\right)=d_{k-l,m}^l\left(\tfrac{1}{2}\pi\right) \quad (37)$$

$$=\frac{(-1)^k}{2^l}\sqrt{\binom{2l}{k}\binom{2l}{l+m}}K_k\left(l+m;\tfrac{1}{2},2l\right). \quad (38)$$

The last form shows that the m-dependence is contained in the square root of the binomial distribution, $\binom{2l}{l+m}$, times the symmetric *Kravchuk* polynomial of degree k in $l+m\in[0,1,\ldots,2l]$.[33] Kravchuks[34] are discrete orthogonal counterparts to the Hermite polynomials [Ref. 35, Eqs. (5.2.13) and (5.2.14)] and binomials to Gaussians.

In Fig. 7 we show the matrix of the Cuernavaca basis. Note that the top states ($k\approx2l$) mirror the bottom states ($k\approx0$) with alternating signs between consecutive points, $\psi_{2l-k}^{(l)}(m)=(-1)^{l-k+m}\psi_k^{(l)}(-m)$. This figure should be compared with Figs. 1, 3, and 5 of the previous bases.

C. Fourier–Kravchuk Transform Matrix
The FrFKT of power α is a rotation around the z axis by an angle $\phi=\frac{1}{2}\pi\alpha$, generated by $\bar{\mathcal{N}}$, which carries the $\bar{\mathcal{Q}}$ x axis onto the $\bar{\mathcal{P}}$ y axis, with a phase [cf. Eq. (2)],

$$\mathcal{K}^\alpha:=\exp\left(-i\tfrac{1}{2}\pi\alpha\bar{\mathcal{N}}\right)=e^{-i\pi l\alpha/2}\exp\left(-i\tfrac{1}{2}\pi\alpha\mathcal{L}_z\right). \quad (39)$$

The FrFKT matrix elements are built as bilinear generating functions of the wave functions in Eq. (38) for $N=2l$

+1, as in Eq. (16); using standard results from angular momentum theory,[32] they can be summed to a closed form,

$$K_{m,m'}^{(l,\alpha)} = \sum_{k=0}^{2l} \psi_k^{(l)}(m) e^{-i\pi k\alpha} \psi_k^{(l)}(m') = i^{m'-m} d_{m,m'}^l \left(\tfrac{1}{2}\pi\alpha\right).$$

(40)

The set of FrFKT matrices form a group $\mathsf{U}(1)_K \subset \mathsf{SU}(2) \subset \mathsf{U}(2l+1)$. However, note that this group does *not* contain the Fourier matrix $\mathbf{F}$ of Eq. (10); instead, for $\alpha=1$, $\mathbf{K}^{(l,1)}$ is the real matrix shown in Fig. 7, multiplied by a circulating phase, as can be seen by comparing Eqs. (40) and (37). Also, the Cuernavaca model is not periodic: In signals of $N=2l+1$ points, $m=\pm l$ are not first neighbors, but the two ends of the signal.

D. Coherent States in su(2)
The ground state of the su(2) finite oscillator is

$$\psi_0^{(l)}(m) = d_{-l,m}^l\left(\tfrac{1}{2}\pi\right) = \frac{1}{2^l}\sqrt{\binom{2l}{l+m}}.$$

(41)

It is even and centered in $m \in [-l,l]$; this we can imagine as a density bump on the south pole of a sphere, which is projected on the position x axis as a discrete Gaussianlike function. Rotation of this sphere around the y axis of momentum through an angle $-\theta$, will translate the projection of its density bump in Eq. (41) along the position axis by $\sin\theta$ [cf. Eq. (7)] without exceeding the interval. The center of the bump reaches the equator at $\theta = \tfrac{1}{2}\pi$ and extends up to the north pole of the sphere for $\theta = \pi$. Similarly, rotation of the sphere around the x axis with $\exp(i\eta\bar{\mathcal{Q}})$ will multiply the signal values by linear phases, and this translates the momentum of the ground state in Eq. (41).

We defined the coherent states of the Cuernavaca model for $0 \le \theta \le \pi$ by

$$\boldsymbol{\kappa}_\theta^{(l)} := \exp(i\theta\bar{\mathcal{P}})\boldsymbol{\psi}_0^{(l)},$$

(42)

$$\kappa_\theta^{(l)}(m) = d_{m,-l}^l\left(-\tfrac{1}{2}\pi - \theta\right)$$

(43)

$$= \sum_{k=0}^{2l} (-1)^k d_{l,l-k}^l(\theta) \psi_k^{(l)}(m),$$

(44)

$$d_{l,l-k}^l(\theta) = \left(\cos\tfrac{1}{2}\theta\right)^l \sqrt{\binom{2l}{k}} \left(\sin\tfrac{1}{2}\theta\right)^k.$$

(45)

Equation (43) follows from angular momentum theory,[32] and Eq. (44) displays coherent states as the linear generating function of the number eigenvector set $\psi_k^{(l)}(m)$ [cf. Eqs. (8) and (21)]; however, the coefficients of the truncated exponential series $c^k/\sqrt{k!}$ are here replaced by Eq. (45) as $\sim(\sin\tfrac{1}{2}\theta)^k/\sqrt{k!(2l-k)!}$.

The FrFKT in Eq. (39) will rotate the sphere around the z axis by $\phi = \tfrac{1}{2}\pi\alpha$, so the Gaussian bump projection on the x axis of $\boldsymbol{\kappa}_\theta^{(l)}$ will oscillate harmonically with α modulo 4, while the coherent state parameter $c(0,\theta) := \sin\tfrac{1}{2}\theta$ in Eq. (45) is multiplied by a phase, $c(\phi,\theta)$
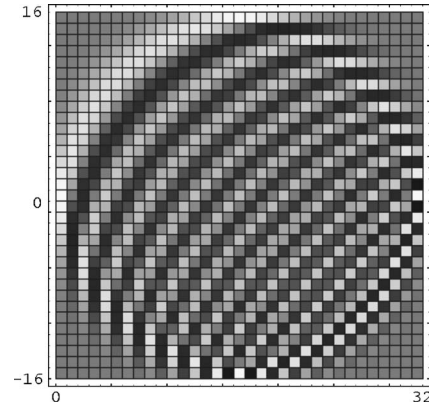

Fig. 7. Matrix (m,k) of the Cuernavaca discrete wave functions of the finite oscillator, $\psi^k(m)$ in Eq. (37), for $l=16$ ($N=33$). See the $m \leftrightarrow m$ and $k \leftrightarrow 2l-k$ parity covariances with the signs $(-1)^k$ and $(-1)^{l-k+m}$, respectively.
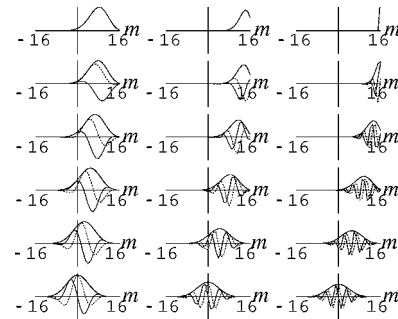

Fig. 8. Motion of the coherent states $\kappa_\theta^{(l)}$ in Eqs. (42)–(45) under fractional Fourier–Kravchuk transformations. In the three columns, $\theta=30°$, $60°$, and $90°$. The rows have the same parameters as those in Figs. 2, 4, and 6.

$:= \exp(-i\tfrac{1}{2}\pi\alpha)c(0,\theta)$, which is the exact analog of Eqs. (9) and (21). The basic commutator here is $[\bar{\mathcal{Q}},\bar{\mathcal{P}}]=i(\bar{\mathcal{N}}-l\mathbf{1})$ instead of the standard quantum mechanical $[\mathcal{Q},\mathcal{P}]=i\mathbf{1}$. In Fig. 8 we show the motion of Cuernavaca coherent states over one-quarter Fourier cycles.

E. Phase Space of Discrete Systems
The Cuernavaca model is based on the manifold of the Lie algebra su(2) with the operators of Eqs. (33)–(35). A proper covariant Wigner distribution is a function of $(q,p,n) \in \mathsf{R}^3$ that we called *meta*-phase space.[36,37] An N-point discrete system belongs to the spin-l representation ($N=2l+1$), whose Casimir [Eq. (36)] classically reduces the manifold to a sphere of radius $\approx l$, which is an easily visualized symplectic manifold. Tangent to the south pole is ordinary phase space $(q,p) \in \mathsf{R}^2$. Evolution along the harmonic guide (modulo a "metaplectic" phase) is rotation of the sphere around its vertical axis; prisms rotate the sphere around its y axis; inclined slabs translate signals in x, across the guide and with "reflection" at the endpoints. Consideration of transformations generated by elements in the universal enveloping algebra of su(2) allow for the introduction of aberrations on the phase space of complex signals, such as those due to the Kerr effect.[38]

7. CONCLUSION

It should be interesting to compare the different versions of the FrDFT with the actual output of a planar optical Fourier signal processor, particularly a waveguide, at finite linear arrays of sensors. We expect that in such guides, well-collimated coherent beams will evolve with close-to-harmonic motion. Then we could select a "best" *V*-basis so that its *V*-FrDFT approximates the close-to-Fourier action of that particular signal processor.

ACKNOWLEDGMENTS

REFERENCES

1. E. U. Condon, "Immersion of the Fourier transform in a continuous group of functional transformations," Proc. Natl. Acad. Sci. U.S.A. **23**, 158–164 (1937).
2. M. Moshinsky and C. Quesne, "Oscillator systems," in *Proceedings of the 15th Solvay Conference in Physics (1970)* (Gordon and Breach, 1974).
3. K. B. Wolf, *Integral Transforms in Science and Engineering* (Plenum, 1979).
4. S. A. Collins Jr., "Lens-system diffraction integral written in terms of matrix optics," J. Opt. Soc. Am. **60**, 1168–1177 (1970).
5. H. M. Ozaktas, Z. Zalevsky, and M. Alper Kutay, *The Fractional Fourier Transform with Applications in Optics and Signal Processing* (Wiley, 2001).
6. N. M. Atakishiyev and K. B. Wolf, "Fractional Fourier–Kravchuk transform," J. Opt. Soc. Am. A **14**, 1467–1477 (1997).
7. A. W. Lohmann, "Image rotation, Wigner rotation, and the fractional order Fourier transform," J. Opt. Soc. Am. A **10**, 2181–2186 (1993).
8. D. Mendlovich and H. M. Ozaktas, "Fourier transforms of fractional order and their optical interpretation," Opt. Commun. **101**, 163–169 (1993).
9. H. M. Ozaktas, O. Aríkan, M. A. Kutay, and G. Bozdagí, "Digital computation of the fractional Fourier transform," IEEE Trans. Signal Process. **44**, 2141–2150 (1996).
10. S.-C. Pei and M.-H. Yeh, "Improved discrete fractional transform," Opt. Lett. **22**, 1047–1049 (1997).
11. S.-C. Pei, M.-H. Yeh, and C.-C. Tseng, "Discrete fractional Fourier transform based on orthogonal projections," IEEE Trans. Signal Process. **47**, 1335–1348 (1999).
12. M. L. Mehta, "Eigenvalues and eigenvectors of the finite Fourier transform," J. Math. Phys. **28**, 781–785 (1987).
13. Ç. Candan, M. Alper Kutay, and H. M. Ozaktas, "The discrete fractional Fourier transform," IEEE Trans. Signal Process. **48**, 1329–1337 (1999).
14. L. Barker, Ç. Candan, T. Hakioğlu, A. Kutay, and H. M. Ozaktas, "The discrete harmonic oscillator, Harper's equation, and the discrete fractional Fourier transform," J. Phys. A **33**, 2209–2222 (2000).
15. N. M. Atakishiyev, L. E. Vicent, and K. B. Wolf, "Continuous vs. discrete fractional Fourier transforms," J. Comput. Appl. Math. **107**, 73–95 (1999).
16. N. M. Atakishiyev, G. S. Pogosyan, and K. B. Wolf, "Finite models of the oscillator," Phys. Part. Nucl. **36**, 521–555 (2005).
17. K. B. Wolf, *Geometric Optics on Phase Space* (Springer-Verlag, 2004).
18. V. Namias, "The fractional order Fourier transform and its application to quantum mechanics," J. Inst. Math. Appl. **25**, 241–265 (1980).
19. N. M. Atakishiyev, D. Galetti, and J. P. Rueda, "On relations between certain *q*-polynomial families, generated by the finite Fourier transform," Int. J. Pure Appl. Math. **26**, 275–284 (2006).
20. N. M. Atakishiyev, "On *q*-extensions of Mehta's eigenvectors of the finite Fourier transform," Int. J. Mod. Phys. A **21**, 4993–5006 (2006).
21. T. S. Santhanam and A. R. Tekumalla, "Quantum mechanics in finite dimensions," Found. Phys. **6**, 583–589 (1976).
22. C. Belingeri and P. E. Ricci, "A generalization of the discrete Fourier transform," Integral Transforms Spec. Funct. **3**, 165–174 (1995).
23. M. S. Richman, T. W. Parks, and R. G. Shenoy, "Discrete-time, discrete-frequency analysis," IEEE Trans. Signal Process. **46**, 1517–1527 (1998).
24. M. Shiri-Garakani and D. R. Finkelstein, "Finite quantum mechanics of the harmonic oscillator," J. Math. Phys. **47**, 032105 (2006).
25. T. Opatrný, "Mean value and uncertainty of optical phase space—a simple mechanical analogy," J. Phys. A **27**, 7201–7208 (1994).
26. T. Opatrný, "Number-phase uncertainty relations," J. Phys. A **28**, 6961–6975 (1995).
27. B. W. Forbes and M. A. Alonso, "Measures of spread for periodic distributions and the associated uncertainty relations," Am. J. Phys. **69**, 340–347 (2001).
28. M. A. Alonso and M. J. Bastiaans, "Mapping-based width measures and uncertainty relations for periodic functions," Signal Process. **84**, 2425–2435 (2004).
29. T. Hakioğlu, "Finite dimensional Schwinger basis, deformed symmetries, Wigner function, and an algebraic approach to quantum phase," J. Phys. A **31**, 6975–6994 (1998).
30. T. Hakioğlu, "Linear canonical transformations and quantum phase: a unified canonical and algebraic approach," J. Phys. A **32**, 4111–4130 (1999).
31. T. Hakioğlu and K. B. Wolf, "The canonical Kravchuk basis for discrete quantum mechanics," J. Phys. A **33**, 3313–3323 (2000).
32. L. C. Biedenharn and J. D. Louck, *Angular Momentum in Quantum Physics*, Encyclopedia of Mathematics and Its Applications, Vol. 8, G.-C. Rota, ed. (Addison-Wesley, 1981).
33. N. M. Atakishiyev and S. K. Suslov, "Difference analogs of the harmonic oscillator," Theor. Math. Phys. **85**, 1055–1062 (1991).
34. M. Krawtchouk, "Sur une généralization des polinômes d'Hermite," C. R. Acad. Sci. Paris **189**, 620–622 (1929).
35. A. F. Nikiforov, S. K. Suslov, and V. B. Uvarov, *Classical Orthogonal Polynomials of a Discrete Variable*, Springer Series in Computational Physics (Springer-Verlag, 1991).
36. N. M. Atakishiyev, S. M. Chumakov, and K. B. Wolf, "Wigner distribution function for finite systems," J. Math. Phys. **39**, 6247–6261 (1998).
37. S. T. Ali, N. M. Atakishiyev, S. M. Chumakov, and K. B. Wolf, "The Wigner function for general Lie groups and the wavelet transform," Ann. Inst. Henri Poincare **1**, 685–714 (2000).
38. S. M. Chumakov, A. Frank, and K. B. Wolf, "Finite Kerr medium: macroscopic quantum superposition states and Wigner functions on the sphere," Phys. Rev. A **60**, 1817–1823 (1999).